Proton Lability in Highly Hindered Dinuclear Palladium(I) μ-Phosphido−Secondary Phosphine Complexes. Crystal Structures of $[Pd_2(\mu\text{-}PBu^t_2)(PCy_2H)_3(CO)]BF_4$ and $[Pd_2(\mu\text{-}PBu^t_2)(PCy_2H)_2(\mu,\eta^2,\eta^2\text{-isoprene})]BF_4$

Piero Leoni,*,†,‡ Marco Pasquali,*,† Milena Sommovigo,† Alberto Albinati,*,§ Paul S. Pregosin,*,|| and Heinz Rüegger||

Dipartimento di Chimica e Chimica Industriale, Via Risorgimento 35, I-56126 Pisa, Italy, Scuola Normale Superiore, Piazza dei Cavalieri 7, I-56100 Pisa, Italy, Istituto di Chimica Farmaceutica, Viale Abruzzi 42, I-20131 Milano, Italy, and Inorganic Chemistry, ETH Zentrum, CH-8092 Zürich, Switzerland

Received November 27, 1995[⊗]

The reactions of the dinuclear cationic complexes $[Pd_2(\mu\text{-}PBu^t_2)(PR_3)_4]^+$ ($PR_3 = PCy_2H$, PMe_3) with CO or isoprene proceed with substitution of one or two phosphine ligands giving the corresponding $[Pd_2(\mu\text{-}PBu^t_2)(PR_3)_3(CO)]^+$ and $[Pd_2(\mu\text{-}PBu^t_2)(\mu,\eta^2,\eta^2\text{-isoprene})(PR_3)_2]^+$ cations. $[Pd_2(\mu\text{-}PBu^t_2)(PCy_2H)_3(CO)]^+$ equilibrates in solution to a mixture of monocarbonyl derivatives arising from bridging phosphido/terminal phosphine interchange. The complexes were characterized by multinuclear 1-D and 2-D NMR spectroscopy. The crystal and molecular structures of $[Pd_2(\mu\text{-}PBu^t_2)(PCy_2H)_3(CO)]BF_4$ and $[Pd_2(\mu\text{-}PBu^t_2)(PCy_2H)_2(\mu,\eta^2,\eta^2\text{-isoprene})]CF_3SO_3$ were solved by single-crystal X-ray diffraction studies.

Introduction

Steric crowding around metal centers has proven a powerful tool in the synthesis of new compounds with both low coordination number and a high electron deficiency at the metal.[1] In such compounds the metal center is highly reactive but often inaccessible for sterically demanding reactive ligands. This promotes weak interactions, e.g. agostic interactions with σ bonds of the ligands,[2] provided empty orbitals of suitable symmetry are available at the metal. Ligand discrimination and eventually activation based on its dimensions can also be effective.[3] This can, in principle, be exploited in the selective coordination of small molecules in the presence of larger ones, even if the latter would be more reactive under normal reaction conditions.

We have recently reported the synthesis[4] of $[Pd_2(\mu\text{-}PBu^t_2)(\mu\text{-}PBu^t_2H)(PBu^t_2H)_2]X$ [(**1**)X, X = BF_4, CF_3SO_3] which are stable in the presence of an excess of PBu^t_2H but react easily[5] with less encumbered phosphines such as PMe_3 or PCy_2H giving $[Pd_2(\mu\text{-}PBu^t_2)(PR_3)_4]X$ [(**2**)$^+$, $PR_3 = PMe_3$; (**3**)$^+$, $PR_3 = PCy_2H$] (Scheme 1).

The reactions of the cations (**2**)$^+$ and (**3**)$^+$ with CO and isoprene and a comparison of these results with those obtained[4b,6] in the analogous reactions of (**1**)$^+$ are now reported. We also describe the interchange of the phosphido and secondary phosphine ligands observed in some of the complexes.

Results and Discussion

Reactions with CO. Either (**2**)CF_3SO_3 or (**3**)BF_4 react under mild conditions with carbon monoxide giving the reversible formation of the monocarbonyl derivatives $[Pd_2(\mu\text{-}PBu^t_2)(PMe_3)_3(CO)]CF_3SO_3$, (**4**)$CF_3SO_3$, and $[Pd_2(\mu\text{-}PBu^t_2)(PCy_2H)_3(CO)]BF_4$, (**5**)$BF_4$ (Scheme 1). The complexes were isolated in good yields as yellow crystalline solids and represent two relatively rare examples of Pd(I) complexes with terminal CO ligands. Both complexes were characterized by spectroscopic means, and the crystal structure of (**5**)BF_4 was solved by diffraction methods (see below). The complexes exhibit a single CO stretching absorbtion in the IR spectrum [ν_{CO} at 2015, (**4**)$^+$, and 2017 cm^{-1}, (**5**)$^+$]; these frequencies are unusually low[7] for terminal Pd−CO ligands, suggesting significant π-back-bonding, despite the cationic nature of the derivatives. Complex (**5**)BF_4 equilibrates in solution to a mixture of isomers, and their NMR characterization will be described in the next section. The $^{31}P\{^1H\}$ NMR spectrum (CD_2Cl_2, 273 K)

† Dipartimento di Chimica e Chimica Industriale.
‡ Scuola Normale Superiore.
§ Istituto di Chimica Farmaceutica.
|| ETH Zentrum.
⊗ Abstract published in *Advance ACS Abstracts,* March 15, 1996.

(1) (a) Covert, K. J.; Neithamer, D. R.; Zonnevylle, M. C.; La Pointe, R. E.; Schaller, C. P.; Wolczanski, P. T. *Inorg. Chem.* **1991**, *30*, 2494. (b) Chen, H.; Bartlett, R. A.; Dias, H. V. R.; Olmstead, M. M.; Power, P. P. *Inorg. Chem.* **1991**, *30*, 2487. (c) Arduengo, A. J., III; Gamper, S. F.; Calabrese, J. C.; Davidson, F. *J. Am. Chem. Soc.* **1994**, *116*, 4391. (d) Wolf, J. R.; Bazan, G. C.; Schrock, R. R. *Inorg. Chem.* **1993**, *32*, 4155. (e) Hermes, A. R.; Girolami, G. S. *Inorg. Chem.* **1988**, *27*, 1775.

(2) (a) Wasserman, H. J.; Kubas, G. J.; Ryan, R. R. *J. Am. Chem. Soc.* **1986**, *108*, 2294. (b) Gonzales, A. A.; Zhang, K.; Hoff, C. D. *Inorg. Chem.* **1989**, *28*, 4285. (c) Matsumoto, M.; Yoshioka, H.; Nakatsu, K.; Yoshida, T.; Otsuka, S. *J. Am. Chem. Soc.* **1974**, *96*, 3322.

(3) Campion, B. K.; Heyn, R. H.; Tilley, T. D. *J. Chem. Soc., Chem. Commun.* **1992**, 1201.

(4) (a) Albinati, A.; Lianza, F.; Pasquali, M.; Sommovigo, M.; Leoni, P.; Pregosin, P. S.; Rüegger, H. *Inorg. Chem.* **1991**, *30*, 4690. (b) Leoni, P.; Pasquali, M.; Sommovigo, M.; Laschi, F.; Zanello, P.; Albinati, A.; Lianza, F.; Pregosin, P. S.; Rüegger, H. *Organometallics* **1993**, *12*, 1702.

(5) Leoni, P.; Pasquali, M.; Sommovigo, M.; Laschi, F.; Zanello, P.; Albinati, A.; Lianza, F.; Pregosin, P. S.; Rüegger, H. *Organometallics* **1994**, *13*, 4017.

(6) Leoni, P.; Pasquali, M.; Sommovigo, M.; Laschi, F.; Zanello, P.; Albinati, A.; Lianza, F.; Pregosin, P. S.; Rüegger, H. *Organometallics* **1993**, *12*, 4503.

(7) Wang, C.; Willner, H.; Bodenbinder, M.; Batchelor, R. J.; Einstein, F. W. B.; Aubke, F. *Inorg. Chem.* **1994**, *33*, 3521.

0276-7333/96/2315-2047$12.00/0

Scheme 1

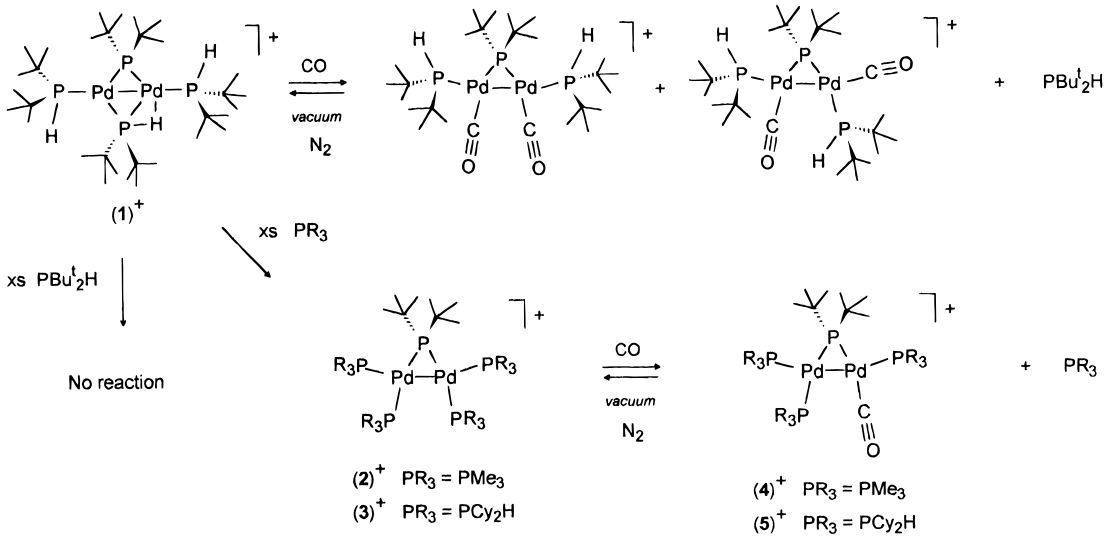

Table 1. ^{31}P NMR Parameters of Carbonyl Complexes[a]

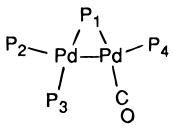

	$\delta(P_1)$	$\delta(P_2)$	$\delta(P_3)$	$\delta(P_4)$	$^2J_{12}$	$^2J_{13}$	$^2J_{14}$	$^2J_{23}$	$^3J_{24}$	$^3J_{34}$
(**4**)$^{+\,b}$	339.5	21.1	−26.2	−32.6	43	227	12	51	187	16
(**5**)$^{+\,c}$	347.1	−2.3	17.8	−3.9	32	201	9	41	159	
(**6**)$^{+\,c}$	341.8	−3	16.5	35.0	34	200	8	40	151	
(**7**)$^{+\,c}$	299.3	10.0	20.8	−3.9	35	205			166	
(**8**)$^{+\,c}$	295.5	7.7	19.5	35.8	39	200		39	158	

[a] Chemical shifts are relative to H_3PO_4, and coupling constants are in Hz. [b] CD_2Cl_2 solution at 81 MHz and 273 K. [c] Recorded in acetone-d_6 solution at 202 MHz and room temperature.

of (**4**)CF_3SO_3 is consistent with the structure drawn in Scheme 1. The spectrum exhibits a slightly broadened doublet of doublets at 340 ppm (J_{PP} = 227 and ca. 40 Hz) for the bridging phosphido ligand. The larger coupling confirms the presence of one coordinated PMe_3 molecule pseudo-*trans* to the phosphido ligand. The presence of two smaller unresolved *cis* $^2J_{PP}$ couplings can be determined from the sharper PMe_3 absorptions. These consist of three well-resolved eight-line multiplets at −21.1, −26.2, and −32.6 ppm, which were assigned, respectively, to P(2), P(3), and P(4) (see Table 1).

The different behavior of the cation (**1**)$^+$, with respect to (**2**)$^+$ and (**3**)$^+$, in the reaction with CO should be emphasized. Under identical experimental conditions the former gives[4b] a mixture of two isomeric dicarbonyls of formula $[Pd_2(\mu\text{-}PBu^t_2)(PBu^t_2H)_2(CO)_2]^+$ while (**2**)$^+$ and (**3**)$^+$ give only the corresponding monocarbonyl derivatives (**4**)$^+$ and (**5**)$^+$, respectively, with no tendency to further carbonylation (Scheme 1). This observation, together with the unsuccessful attempt to form[5] the PBu^t_2H analogue of the cations (**2**)$^+$ and (**3**)$^+$ by reacting (**1**)$^+$ with a large excess of PBu^t_2H (Scheme 1), confirms that two molecules of PBu^t_2H are too large to be coordinated terminally to the same metal center of the $Pd_2(\mu\text{-}PBu^t_2)$ core.

Isomerization of the Cation (5)$^+$. Consistent with the single carbonyl absorption at 2017 cm^{-1}, and confirmed by the crystal structure determination, the solid samples of (**5**)$^+$ contain a single isomer. However, the solution chemistry of (**5**)$^+$ proved unexpectedly complicated. The $^{31}P\{^1H\}$ NMR spectrum in acetone-d_6 showed at least six absorptions in the bridging phosphide region between ca. 180 and 460 ppm. The relative intensities of these signals changed over a period of hours and eventually reached an equilibrium in which two main components remained. Of the six original high-frequency resonances, four were eventually assigned to the complexes (**5**)$^+$−(**8**)$^+$, with (**5**)$^+$ the most prominent immediately after solution (Chart 1).

Chart 1

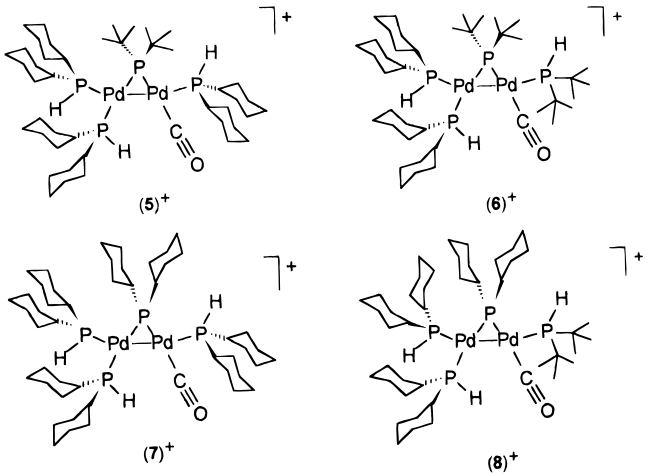

We believe that the two unassigned, rather weak, high-frequency signals arise from a complex with a bridging secondary PHR_2 ligand, structurally analogous to the previously described cation (**1**)$^+$.[4,5] The low-frequency ^{31}P region (between ca. δ = −4 and +40) was complicated due to the fact that each complex gives three nonequivalent ^{31}P signals for the terminal phosphines. We give a summary of the various ^{31}P parameters in Table 1. The assignments were based on empiricisms derived from our previous studies together with 2-D exchange spectroscopy. Note that the bridging PBu^t_2 ligands appear at much higher frequencies than the bridging PCy_2 ligands; this empirical observation is also valid in the low-frequency region (see Table 1). Moreover, the various ^nJ(P,P) were important in the assignments, since the pseudo-*trans* spin−spin cou-

plings $^2J(P_1,P_3)$ (ca. 200 Hz) and $^3J(P_2,P_4)$ (ca. 160 Hz) are both much larger than the other couplings.

After 24 h the solution contains mostly $(\mathbf{8})^+$; i.e. complex $(\mathbf{5})^+$ has isomerized to its thermodynamically more stable isomer with a μ^2-PCy_2 group and a terminal $PHBu^t_2$ ligand. This type of exchange is not totally unprecedented[5] and could arise in our complexes via initial loss of the CO ligand, followed by formation of the intermediate (**A**) with a bridging secondary phosphine (eq 1, L = CO); as described previously.[5] Complex $(\mathbf{3})^+$ behaves similarly (eq 1, L = PCy_2H).

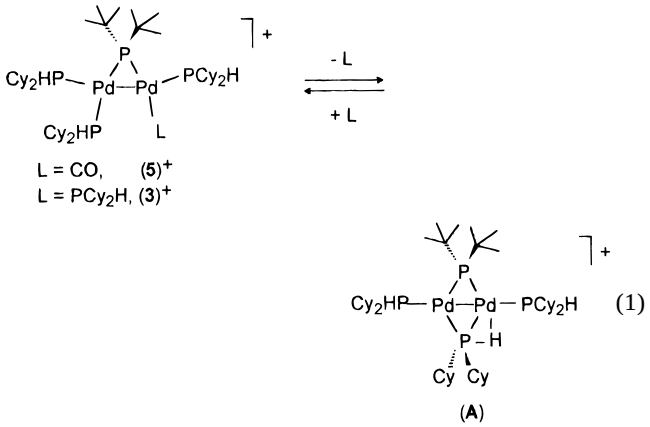

Either intra- or intermolecular H migration in **A** from the bridging PCy_2H molecule to the μ-PBu^t_2 ligand, followed by recoordination of CO, would provide the isomerization of $(\mathbf{5})^+$ to $(\mathbf{8})^+$.

It is obvious from structures $(\mathbf{5})^+$−$(\mathbf{8})^+$ that these complexes can dissociate one or more of the terminal phosphines. This is clearly indicated by the presence of the redistribution products $(\mathbf{6})^+$ and $(\mathbf{7})^+$, which reveal *two* Bu^t- and *four* Cy-containing phosphorus ligands, respectively. Moreover, there is, at least, another dynamic process which selectively exchanges the pseudo-*trans* terminal secondary phosphine ligands (indicated as spins P_2 and P_4 in Table 1) in $(\mathbf{5})^+$ and $(\mathbf{7})^+$, as shown via 2-D ^{31}P exchange NMR (see Figure 1).

The latter process could arise via the same intermediate **A** discussed above. Re-formation of a coordinated terminal secondary phosphine, this time at the Pd atom which previously held the CO, and renewed CO complexation rationalizes the selective P_2,P_4 exchange (Scheme 2). However this could be accomplished also by other routes, i.e. (a) direct 1,2-PCy_2H shift from **X** to **X′**, (b) intermediate intramolecular H migration from **A** to **A′**, (c) intermolecular H^+ exchange, and (d) dissociation and recoordination of PCy_2H molecules 2 and 4.

What is obvious from the whole of our results is that several ligands can dissociate and the PH hydrogen atom of at least one secondary phosphine can easily migrate, thus explaining the observation of a relatively large number of compounds in solution. In this particular case, it was advantageous to have P-donors with different substitutents in $(\mathbf{5})^+$, as it, unexpectedly, provided insight into the solution dynamics of our materials.

Reactions with Isoprene. Complexes $(\mathbf{2})CF_3SO_3$ and $(\mathbf{3})CF_3SO_3$ react with isoprene giving high yields of the yellow crystalline derivatives $[Pd_2(\mu\text{-}PBu^t_2)(PR_3)_2(\mu,\eta^2,\eta^2\text{-}trans\text{-}CH_2{=}C(Me)CH{=}CH_2)]CF_3SO_3$

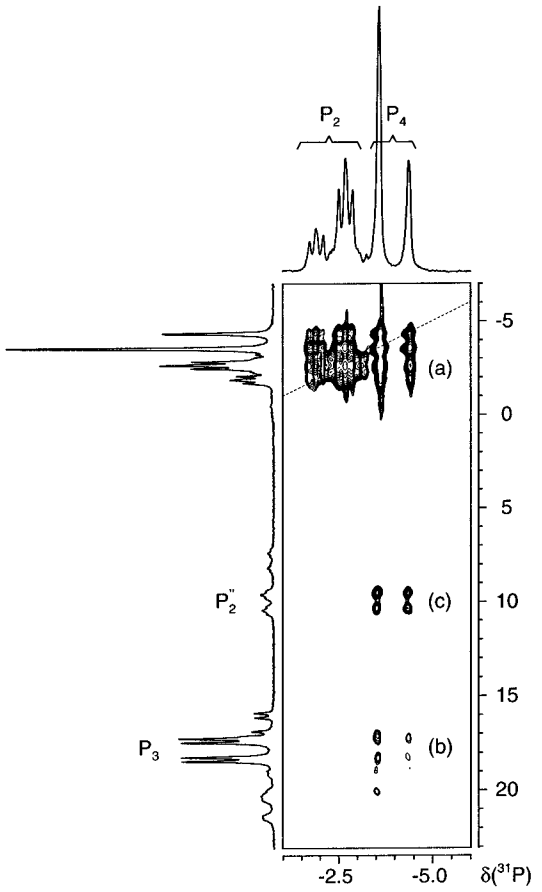

Figure 1. Section of the two-dimensional ^{31}P exchange spectrum (202 MHz, acetone-d_6, room temperature, t_{mix} = 400 ms) showing exchange between the P_4 and P_2 (a) and P_4 and P_3 (b) sites in $(\mathbf{5})^+$ and positions P_4 and P_2 (c) in $(\mathbf{7})^+$, respectively. Note that the cross-peaks for the exchange of P_4 and P_2 lie very close to the diagonal.

[$(\mathbf{9})CF_3SO_3$, $PR_3 = PMe_3$; $(\mathbf{10})CF_3SO_3$, $PR_3 = PCy_2H$; eq 2], in strict analogy to the reaction of $(\mathbf{1})^+$ with isoprene.[6]

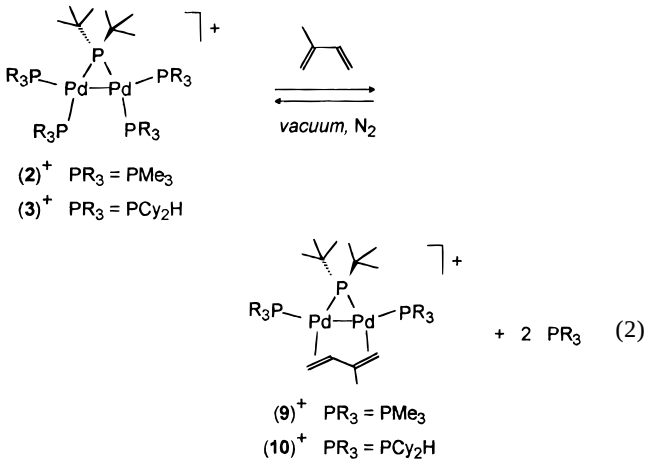

The main features of the NMR spectra of the isoprene complexes (see Experimental Section) are analogous to those of $[Pd_2(\mu\text{-}PBu^t_2)(PBu^t_2H)_2(\mu,\eta^2,\eta^2\text{-}trans\text{-}CH_2{=}C(Me)CH{=}CH_2)]CF_3SO_3$,[6] $(\mathbf{11})CF_3SO_3$, and will not be discussed further.

The reactions of the cations $(\mathbf{1})^+$, $(\mathbf{2})^+$, and $(\mathbf{3})^+$ with isoprene provide the same type of product, with no observed effect of the bulkiness of the phosphine. This may be due to the features of the diene, which favor

Scheme 2

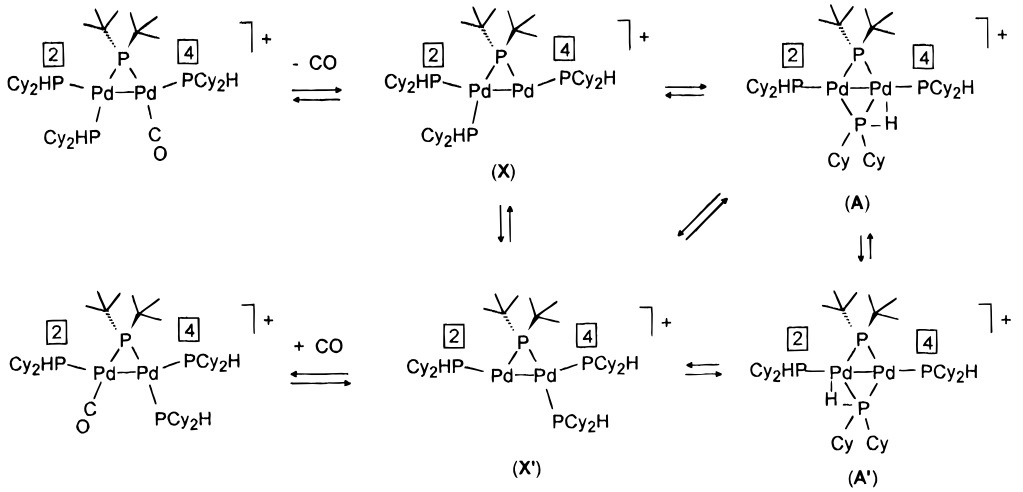

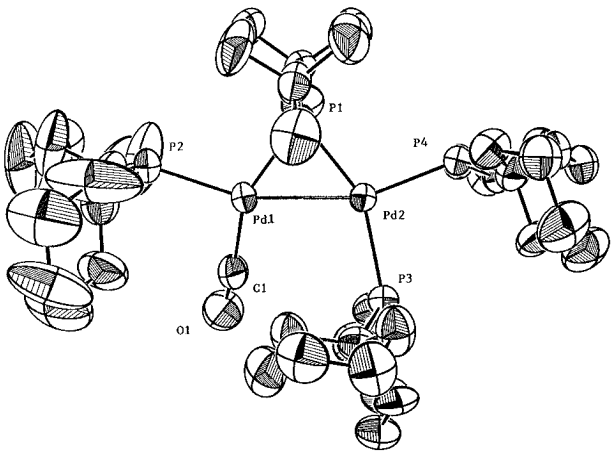

Figure 2. ORTEP plot of the cation $(\mathbf{5})^+$, with the atom-numbering scheme.

Table 2. Selected Bond Distances (Å) and Angles (deg) for $(\mathbf{5})BF_4$ and $(\mathbf{10})CF_3SO_3$ (Esd's in Parentheses)

	$(\mathbf{5})BF_4$	$(\mathbf{10})CF_3SO_3$
Pd(1)−Pd(2)	2.7436(5)	2.713(2)
Pd(1)−P(1)	2.272(2)	2.260(6)
Pd(1)−P(2)	2.341(1)	2.280(5)
Pd(2)−P(1)	2.260(2)	2.253(6)
Pd(2)−P(3)	2.361(2)	2.280(5)
Pd(2)−P(4)	2.316(1)	
Pd(1)−C(1)	1.940(8)	2.24(2)
Pd(1)−P(1)−Pd(2)	74.50(5)	73.9(2)
P(1)−Pd(1)−Pd(2)	52.55(4)	52.9(1)
P(1)−Pd(2)−Pd(1)	52.95(4)	53.2(1)
P(1)−Pd(1)−P(2)	106.75(6)	110.8(2)
P(2)−Pd(1)−C(1)	99.7(2)	90.5(5)
P(3)−Pd(2)−C(4)		94.5(5)
P(1)−Pd(2)−P(4)	106.70(6)	
P(3)−Pd(2)−P(4)	99.69(5)	

the formation of chelate rather than monoolefin-bonded derivatives. Differences were observed in the reactivity of the isoprene complexes; in fact while CO reacts promptly and reversibly with the *tert*-butyl derivative $(\mathbf{11})^+$ to give $[Pd_2(\mu\text{-}PBu^t_2)(PBu^t_2H)_2(CO)_2]^+$, the analogous reactions with $(\mathbf{9})^+$ or $(\mathbf{10})^+$ are much slower. This can be reasonably attributed to the greater bulkiness of the PBu^t_2H ligands.

It should also be pointed out that solutions of complex $(\mathbf{10})CF_3SO_3$ are stable, giving no evidence of the μ-PR_2/PR'_2H exchange described above for $(\mathbf{5})^+$. This stability suggests that a coordinated secondary phosphine does not readily transfer the P−H hydrogen to the pseudo-*cis* bridging phosphide.

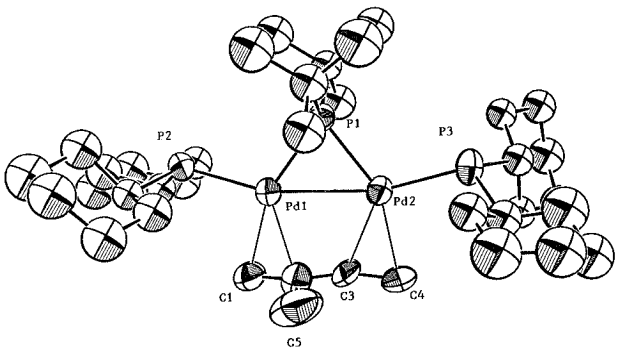

Figure 3. ORTEP plot of the cation $(\mathbf{10})^+$, with the atom-numbering scheme.

Molecular Structures of Complexes $(\mathbf{5})BF_4$ and $(\mathbf{10})CF_3SO_3$. The structure of $(\mathbf{5})BF_4$ was determined by X-ray diffraction, and an ORTEP plot of the molecule is shown in Figure 2; selected bond distances and angles are shown in Table 2. The four phosphorus atoms, the carbonyl carbon, and the two palladium atoms are *not* coplanar. The distortions are such that the pseudo-*trans* $PHCy_2$ ligands, P(2) and P(3), are on opposite sides of the least-squares plane defined by Pd(1), Pd(2), P(1), and P(4) by ca. −0.49 and +0.25 Å, respectively. The ligand atom P(4) is on the same side of this plane as P(2), i.e. away from P(3) by 0.07 Å. This type of distortion is not uncommon.

The bond lengths within the immediate coordination spheres of the two Pd atoms are comparable to those found in $[Pd_2(\mu\text{-}PBu_2^t)(PHCy_2)_4]^+$, $(\mathbf{3})^+$, although the Pd−Pd separation in $(\mathbf{5})^+$, 2.7436(5) Å, is significantly shorter than that found in $(\mathbf{3})^+$, 2.834(4) Å. The P(3)−Pd(2)−P(4) angle, 99.65(5)°, presumably arises as a consequence of interligand steric interactions. This angle, and the somewhat longish Pd(2)−P(4) bond distance of 2.316(1) Å, are suggestive of where this cation might develop dynamic character.

We also managed to obtain suitable crystals of $(\mathbf{10})$-CF_3SO_3, the $PHCy_2$ dinuclear analog of our previously reported $[Pd_2(\mu\text{-}PBu_2^t)(PHBu_2^t)_2(\text{isoprene})]^+$ cation, $(\mathbf{11})^+$. An ORTEP view of the cation $(\mathbf{10})^+$ is shown in Figure 3, and selected bond distances and angles are shown in

Table 2. A comparison of the bond lengths in $(\mathbf{11})^+$ with those of $(\mathbf{10})^+$ reveals that $(\mathbf{10})^+$ is slightly compressed; e.g. the Pd−Pd separation in $(\mathbf{10})^+$ is 2.713(2) Å, and that for $(\mathbf{11})^+$, 2.751(2) Å. There are, however, no major structural differences between the two cations. If one defines a plane using P(1), P(2), Pd(1), and Pd(2), then one finds that these four atoms are almost co-planar, in contrast to our observations for $(\mathbf{5})^+$.

Experimental Section

General Data. All manipulations were carried out under a nitrogen atmosphere using standard Schlenk techniques. Complexes $[Pd_2(\mu\text{-}PBu^t_2)(PCy_2H)_4]X$ and $[Pd_2(\mu\text{-}PBu^t_2)(PMe_3)_4]X$ were prepared as previously described.[5] PCy_2H was purchased from Argus Chemicals and used as received. Solvents were dried by conventional procedures and distilled prior to use. IR spectra (Nujol mull, KBr plates) were recorded on a Perkin-Elmer FT-IR 1725X spectometer. NMR spectra were measured on an AMX500 as described previously.[4−6] Elemental analyses are from the Microanalyses Laboratory of the Faculty of Pharmacy, Pisa, Italy.

Preparation of $[Pd_2(\mu\text{-}PBu^t_2)(PMe_3)_3(CO)]CF_3SO_3$, (4)-$CF_3SO_3$. A red solution of $[Pd_2(\mu\text{-}PBu^t_2)(PMe_3)_4]CF_3SO_3$ (129 mg, 0.159 mmol) in DME (10 mL) was saturated with CO. The solution was left overnight at room temperature and became orange-yellow. An orange solid precipitated after addition of Et_2O (20 mL). The suspension was cooled 3 h at −30 °C, and the precipitate was isolated by filtration and *vacuum* dried yielding 66 mg (0.086 mmol, 54%) of $(\mathbf{5})CF_3SO_3$. Anal. Calcd for $C_{19}H_{45}F_3O_4P_4Pd_2S$: C, 29.8; H, 5.94. Found: C, 30.1; H, 6.01. IR (Nujol, KBr): 2014 vs (ν_{CO}), 1271 vs, 1150 vs, 1031 s, 638 m (uncoordinated triflate) cm^{-1}. NMR (CD_2Cl_2, 273 K): $^{31}P\{^1H\}$, 340 (br dd, $^2J_{PP} = 227$, $^2J_{PP} = 43$ Hz), −21.1 (ddd, $^2J_{PP} = 51$, $^2J_{PP} = 43$, $^3J_{PP} = 187$ Hz), −26.2 (ddd, $^2J_{PP} = 51$, $^2J_{PP} = 227$, $^3J_{PP} = 11.5$ Hz), −32.6 ppm (ddd, $^2J_{PP} = 11.5$, $^3J_{PP} = 11.5$, $^3J_{PP} = 187$ Hz).

Preparation of $[Pd_2(\mu\text{-}PBu^t_2)(PCy_2H)_3(CO)]BF_4$, (5)$BF_4$. $[Pd_2(\mu\text{-}PBu^t_2)(PCy_2H)_4]BF_4$ (191 mg, 0.154 mmol) was suspended in DME (15 mL). The reaction flask was evacuated and filled with CO. The orange suspension turned immediately to yellow, and the solid dissolved after stirring 5 min. The solution was concentrated to ca. 5 mL, and Et_2O (10 mL) was added. After being cooled at −30 °C overnight, the suspension was filtered and the solid product *vacuum* dried (yield: 125 mg, 0.117 mmol, 76%). Anal. Calcd for $C_{45}H_{87}BF_4OP_4Pd_2$: C, 50.6; H, 8.21. Found: C, 50.2; H, 8.03. IR (Nujol, cm^{-1}): 2312 (w), ν(PH); 2017 (vs), ν(CO); 1056 (vs), ν(BF). See text for NMR spectral data.

Preparation of $[Pd_2(\mu\text{-}PBu^t_2)(\mu,\eta^2,\eta^2\text{-}CH_2{=}C(CH_3)\text{-}CH{=}CH_2)(PMe_3)_2]CF_3SO_3$, (9)$CF_3SO_3$. Isoprene (3 mL) was added to a solution of $[Pd_2(\mu\text{-}PBu^t_2)(PMe_3)_4]CF_3SO_3$ (100 mg, 0.123 mmol) in DME (10 mL). After 5 d at room temperature Et_2O (25 mL) was added to the orange solution. The yellow solid which precipitated was isolated by filtration and vacuum dried (49 mg, 0.067 mmol, 54%). Anal. Calcd for $C_{20}H_{44}F_3O_3P_3Pd_2S$: C, 33.0; H, 6.10. Found: C, 33.0; H, 6.45. NMR (CD_2Cl_2), 293 K): $^{31}P\{^1H\}$, 358.6 (dd, $^2J_{PP} = 32.8$, $^2J_{PP} = 32.8$ Hz, μ-*P*), −21.7 (dd, $^2J_{PP} = 32.8$, $^3J_{PP} = 61.6$ Hz, *P*Me_3), −23.1 ppm (dd, $^2J_{PP} = 32.8$, $^3J_{PP} = 61.6$ Hz, *P*Me_3); ^1H, δ 4.20 (t, 1H) 3.60 (m, 1H) 3.06 (ddt, 1H) 2.99 (d, 1H) 2.81 (dd, 1H) (=CH), 1.83 (d, $^2J_{PH} = 8.5$ Hz, PMe_3), 1.81 (d, $^2J_{PH} = 8.3$ Hz, PMe_3), 1.20 (d, $^3J_{PH} = 14.3$ Hz, 9H, C_4H_9), 1.18 (d, $^3J_{PH} = 14.0$ Hz, 9H, C_4H_9), 0.64 (s, 3H, =CCH_3).

Preparation of $[Pd_2(\mu\text{-}PBu^t_2)(\mu,\eta^2,\eta^2\text{-}CH_2{=}C(CH_3)\text{-}CH{=}CH_2)(PCy_2H)_2]CF_3SO_3$, (10)$CF_3SO_3$. $[Pd_2(\mu\text{-}PBu^t_2)(PCy_2H)_4]CF_3SO_3$ (113 mg, 0.087 mmol) was suspended in DME (10 mL), and isoprene (2 mL) was added under stirring. The suspension turned immediately from orange to bright yellow, and the solid dissolved in 10 min. Et_2O (25 mL) was added and the solution cooled at −30 °C overnight. The yellow cristals were isolated by filtration and vacuum dried (yield 57 mg, 0.059 mmol, 68%) Anal. Calcd for $C_{38}H_{72}F_3O_3P_3Pd_2S$: C, 47.0; H, 7.47. Found: C, 47.1; H, 7.72. IR (Nujol, cm^{-1}): 1279 (vs), 1145 (vs), 1032 (vs), 636 (s) (uncoordinated triflate). NMR (CD_2Cl_2, 293 K): $^{31}P\{^1H\}$, δ 377.6 (dd, $^2J_{PP} = 27.7$, $^2J_{PP} = 25.1$ Hz, μ-*P*), 7.5 (dd, $^2J_{PP} = 25.1$, $^3J_{PP} = 55.3$ Hz, *P*Cy_2H), 6.0 ppm (dd, $^2J_{PP} = 27.7$, $^3J_{PP} = 55.3$ Hz, *P*Cy_2H); ^1H, δ 5.33 (dm, $^1J_{PH} = 330.0$ Hz, 1H, P−*H*), 5.30 (dm, $^1J_{PH} = 327.0$ Hz, 1H, P−*H*), 4.78 (dd, $J_{PH} = 2.7$, 2.8 Hz, 1H), 4.03 (ddd, $J_{PH} = 3.1$, 3.4, $J_{HH} = 8.8$ Hz, 1H), 3.30 (ddt, $J_{PH} = 2.1$, 2.1, $J_{HH} = 14.6$, 8.8 Hz, 1H), 3.04 (d, $J_{PH} = 4.5$ Hz, 1H), 2.94 (dd, $J_{PH} = 5.2$, $J_{HH} = 14.6$ Hz, 1H), 1.34 (d, $^3J_{PH} = 14.0$ Hz, 9H, C_4H_9), 1.33 (d, $^3J_{PH} = 14.0$ Hz, 9H, C_4H_9), 2.6, 2.2, 1.9−1.2 (broad signals, 44 H, C_6H_{11}), 0.78 (d, $J_{PH} = 1.3$ Hz, 3H, =CCH_3).

Table 3. Experimental Data for the X-ray Diffraction Study of (5)BF_4 and (10)CF_3 SO_3

	compound	
	(**5**)BF_4	(**10**)CF_3SO_3
formula	$C_{49}H_{84}BF_4P_4Pd_2$	$C_{38}H_{70}F_3O_3P_3Pd_2S$
mol wt	1112.72	969.76
crystal dimens, mm	0.40 × 0.35 × 0.25	0.20 × 0.10 × 0.09
data collcn T, °C	23	23
cryst syst	triclinic	monoclinic
space group	$P\bar{1}$	$P2_1/n$
a, Å	14.412(5)	12.006(1)
b, Å	14.416(3)	22.991(5)
c, Å	15.193(3)	17.327(3)
α, deg	66.89(2)	90
β, deg	72.19(2)	1044.45(2)
γ, deg	77.82 (2)	90
V, Å^3	2749.2(7)	4631.5(9)
Z	2	4
ρ(calcd), g cm^{-3}	1.344	1.391
μ, cm^{-1}	8.045	9.539
radiation (*λ*, Å)	Mo Kα graphite monochromated (0.710 69)	
θ range, deg	2.5 ≤ *θ* ≤ 23.0	2.5 ≤ *θ* ≤ 25.0
scan type	*ω*/2*θ*	*ω*/2*θ*
no. indep data collcd	7923	6980
no. obs refcns (n_o)	5667 ($\|F_o\|^2 > 5.0\sigma(\|F\|^2)$)	2202 ($\|F_o\|^2 > 3.0\sigma(\|F\|^2)$)
R^a	0.043	0.053
$R_w{}^a$	0.058	0.066

[a] $R = \sum(|F_o - (1/k)F_c|)/\sum|F_o|$. $R_w = [\sum w(F_o - (1/k)F_c)^2/\sum w|F_o|^2]^{1/2}$, where $w = [\sigma^2(F_o)]^{-1}$; $\sigma(F_o) = [\sigma^2(F_o^2) + f^4(F_o^2)]^{1/2}/2F_o$.

Crystallography. Crystals suitable for X-ray diffraction of (**5**)BF_4 and (**10**)CF_3SO_3 were obtained by crystallization from DME/ether. Crystals of both compounds were mounted on glass fibers (covered for protection with acrylic resin) at a random orientation on an Enraf-Nonius CAD4 diffractometer for the unit cell and space group determinations and for the data collection. Unit cell dimensions were obtained by least-squares fit of the 2*θ* values of 25 high-order reflections using the CAD4 centering routines. Selected crystallographic and other relevant data are listed in Table 3. For compound (**5**)BF_4 the possibility of a higher cell symmetry, given the equal values of two axes, was also tested; no higher symmetry was found in the diffraction pattern.

Data were measured with variable scan speed to ensure constant statistical precision on the collected intensities. Three standard reflections were used to check the stability of the crystal and of the experimental conditions and measured every 1 h. The orientation of the crystal was checked by measuring three reflections every 300 measurements. Data have been corrected for Lorentz and polarization factors and for decay [compound (**10**)CF_3SO_3] using the data reduction programs of the MOLEN package.[8] Empirical adsorption corrections were applied by using azimuthal (Ψ) scans of three "high-*χ*" angle reflections for both sets of data. The standard

deviations on intensities were calculated in terms of statistics alone, while those on F_o were calculated as shown in Table 3.

The structures were solved by a combination of Patterson and Fourier methods and refined by full-matrix least squares[9] (the function minimized being $\sum[w(F_o - 1/kF_c)^2]$). No extinction correction was found to be necessary. The scattering factors used, corrected for the real and imaginary parts of the anomalous dispersion,[9] were taken from ref 9.

All calculations were carried out using the Enraf-Nonius MOLEN package.[8]

Structural Study of (5)BF_4. A total of 7923 independent data were collected of which 5667 were considered as observed (cf. Table 3) and used for the refinement.

As always in this class of compounds, some of the carbon atoms of the phosphines are found to be disordered (as can be judged by the values of the displacement parameters) resulting in a somewhat large spread of the C−C bond distances. Moreover the BF_4^- counterion was also found to de disordered; therefore an idealized model, based on the strongest peaks in the Fourier difference maps, was constructed and the geometry was kept fixed during the last cycles of refinement.

The refinement was carried out using anisotropic displacement parameters for the atoms of the cation while the B and F atoms were treated isotropically. Upon convergence the final Fourier difference map showed no significant feature.

The contribution of the hydrogen atoms in calculated positions (C−H = 0.95 Å, $B(H) = 1.3B(C_{bonded})$ Å^2) was taken into account but not refined.

(8) *MolEN: Molecular Structure Solution Procedure*; Enraf-Nonius: Delft, The Netherlands, 1990.

(9) *International Tables for X-ray Crystallography*; Kynoch: Birmingham, England, 1974; Vol. IV.

Structural Study of (10)CF_3SO_3. It proved impossible to find good quality crystals of this compound: only a fairly small, weakly diffracting crystal proved to be suitable for the data collection. As a result, only a very limited number of reflections are observed at the 3σ level.

An idealized model for the disordered triflate molecule was constructed, on the basis of the strongest peaks of the difference Fourier map; only the isotropic displacement parameters were refined.

The refinement was carried out, as described above, using anisotropic parameters for the palladium and phosphorus atoms and for the carbons of the isoprene moiety; all other atoms were refined using isotropic displacement parameters.

The contribution of the hydrogen atoms in idealized positions, using the values given previously, was taken into account but not refined. Upon convergence the final Fourier difference map showed no significant feature.

Acknowledgment. Financial support from the Ministero dell'Università e della Ricerca Scientifica e Tecnologica (MURST) and from the CNR (Rome) is gratefully acknowledged.

Supporting Information Available: Tables of complete crystallographic and other relevant data, final atomic and equivalent isotropic displacement parameters, calculated positional and thermal parameters for the hydrogen atoms, anisotropic displacement parameters, and extended bond distances, bond angles, and torsion angles and ORTEP views of the cations (**5**)$^+$ and (**10**)$^+$, showing the complete numbering scheme (35 pages). Ordering information is given on any current masthead page.

OM9509148